Actinic, Spot-Scanning EUV Mask Inspection System

Kenneth C. Johnson kjinnovation@earthlink.net 9/29/2015

Abstract

This paper outlines a design concept for an EUV microscope, which is applicable to actinic photomask inspection in semiconductor manufacture with EUV lithography. The microscope employs a raster-scanned, focused-spot array, using a commercial EUV plasma source and achromatic EUV-transmission microlenses for spot generation.

***

Following is a design concept for an actinic EUV mask inspection system, which operates by raster-scanning an array of discrete, diffraction-limited EUV focus spots over a photomask and detecting the reflected radiation from each spot to synthesize a full-field EUV image. Some advantages of this system are:
(1) The illumination characteristics used for inspection (wavelength, numerical aperture, chief ray angle) can closely match the mask's operational illumination characteristics, ensuring good visibility of relevant defects.
(2) The mask can be inspected through a protective pellicle; there is no need to remove the pellicle.
(3) The imaging resolution is unaffected by the detector pixel size.
(4) The spot-generation optics (EUV microlenses) can be configured to produce diffraction-limited spots on the mask with zero geometric aberration, and can be achromatized to operate with a commercial, broadband EUV source such as the Adlyte system (http://www.adlyte.com/).
(5) A spiral-phase pupil function can be used to greatly enhance defect detection sensitivity.

A schematic of the system is illustrated in Figure 1. Radiation from an EUV source such as the Adlyte LPP (Laser-Produced Plasma) source is directed through spot-generation optics comprising an EUV microlens array, which channels the radiation into separate transmitted beams diverging from discrete source spots on an object plane. (The figure shows edge rays from one particular spot.) A first projection system images the source spots onto corresponding image spots on a reflective EUV mask. The projection system in this configuration is a 3-mirror Offner catoptric system comprising mirrors **M1**, **M2** and **M3**, as described in *Lens Design Fundamentals* by Kingslake, 1978, at page 321. A second projection system, also an Offner 3-mirror system comprising mirrors **M4**, **M5** and **M6** in this configuration, images the mask onto a detector array (e.g. an EUV CCD), each element of which senses reflected radiation from a corresponding source spot. The mask is mechanically scanned across the image spot array in synchronization with the detection to synthesize a high-resolution EUV raster image of the mask surface. A possible scan pattern, illustrating the raster lines traced by individual image spots on the mask, is illustrated in Figure 2.

The Offner system has intrinsically low, but significant, geometric optical aberrations. The point-imaging aberrations can be eliminated by designing the spot-generation optics to produce a perfectly spherical, point-convergent wavefront at each image spot on the mask surface. (The wavefronts are not perfectly spherical at the object plane – the source spots are slightly aberrated to compensate for the first projection system's aberration.) A single microlens element can be designed to produce an aberration-free image spot at one wavelength, but would exhibit chromatic aberration over the 2% wavelength band of an LPP source. However, two microlens elements in series, in the form of a Schupmann doublet as described in U.S. Patent 9,097,983, can simultaneously correct aberrations at two distinct wavelengths. This is adequate to achieve substantially achromatic performance for an LPP source if the microlens focal lengths are sufficiently short.
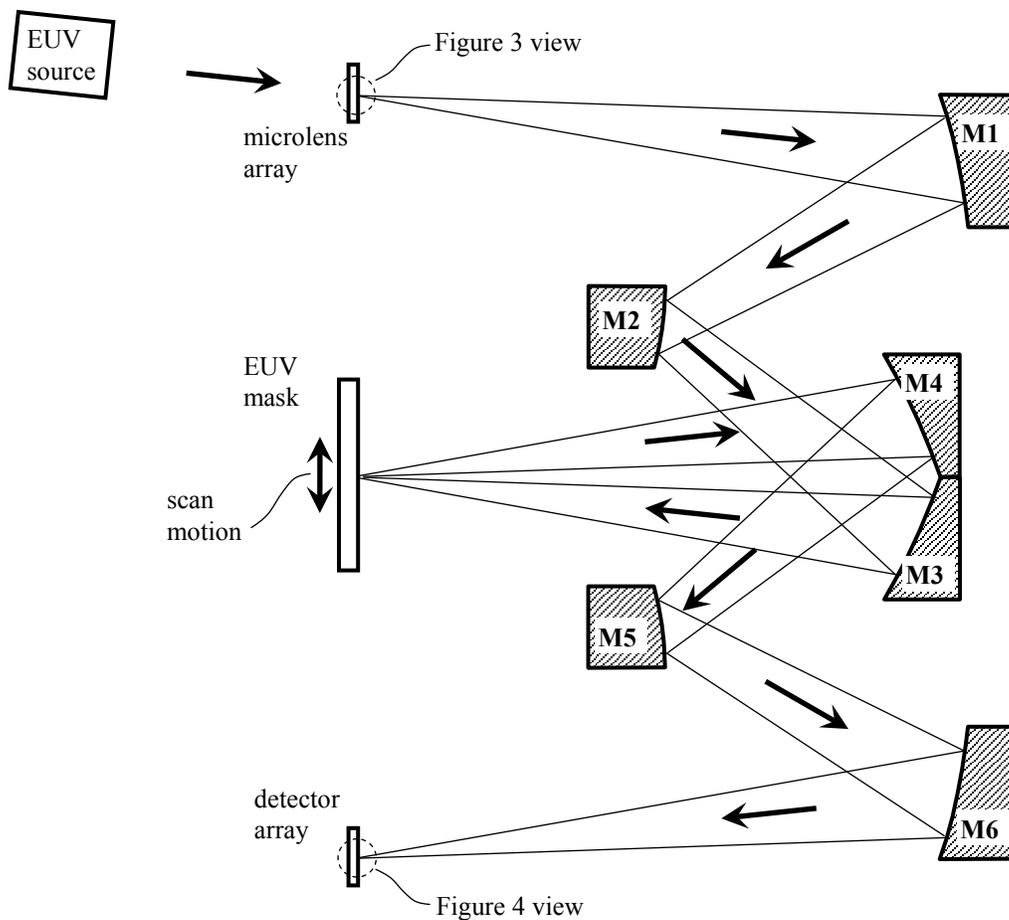

Figure 1. Inspection system schematic.

Figure 3 illustrates an expanded cross section of the microlens array in Figure 1, showing the structure of the Schupmann doublets. (Three doublets and corresponding edge rays are illustrated.) Each doublet comprises a positive-power (converging) element **L1** followed by a negative-power (diverging) element **L2**, with an intermediate lens focus formed between the two elements. The source spots are virtual foci behind the diverging

elements. Both elements are phase-Fresnel molybdenum structures formed on thin silicon substrates. The phase-Fresnel form can be approximated by a multilevel staircase profile, as illustrated by profile **503** in FIG. 5 of U.S. Patent 9,097,983. (The converging element **L1** is concave, and the diverging element **L2** is convex, because the refractive index of molybdenum is less than 1 at EUV wavelengths.) The doublet's EUV transmission efficiency at wavelength 13.5 nm is approximately 36% neglecting substrate losses.
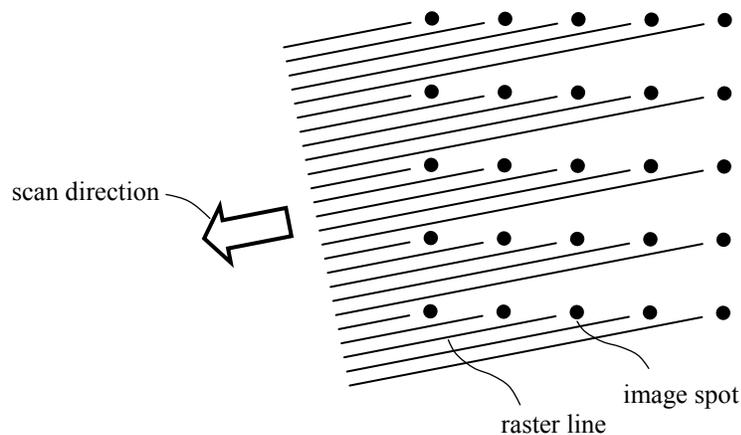

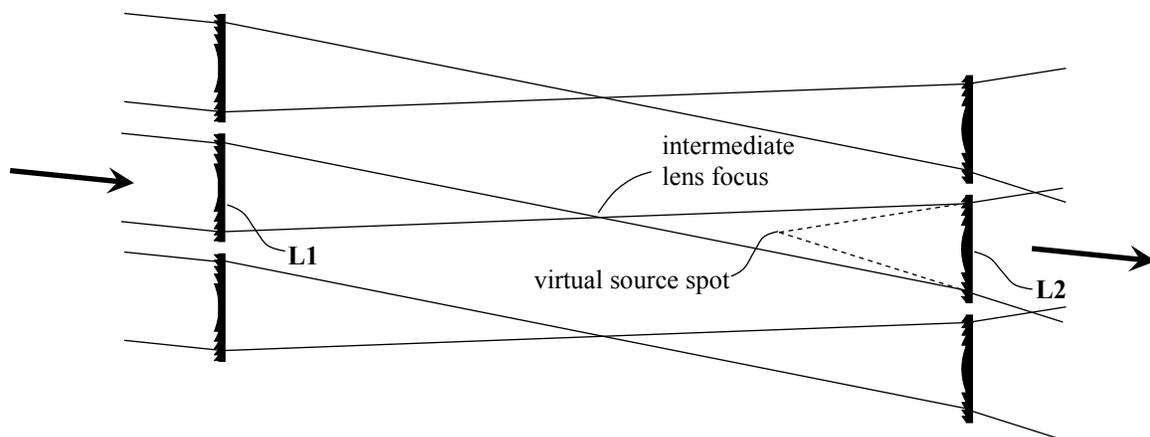Figure 2. Raster scan pattern on mask.

Figure 3. Achromatic Schupmann doublet microlens.

Figure 4 shows an expanded cross section of the detector array in Figure 1. The detector elements can be located anywhere in the space where the individual spot beams are non-overlapping, but preferably not close to the beam foci. The detector elements may be overfilled or underfilled, depending on what portion of the reflected angular spectrum the system is designed to detect. A pinhole could be placed in front of each detector element to limit the captured angular spectrum. Figure 4 illustrates one detector element per spot beam, but it may be advantageous to use multiple detector elements per beam to simultaneously sense different portions of the angular spectrum.
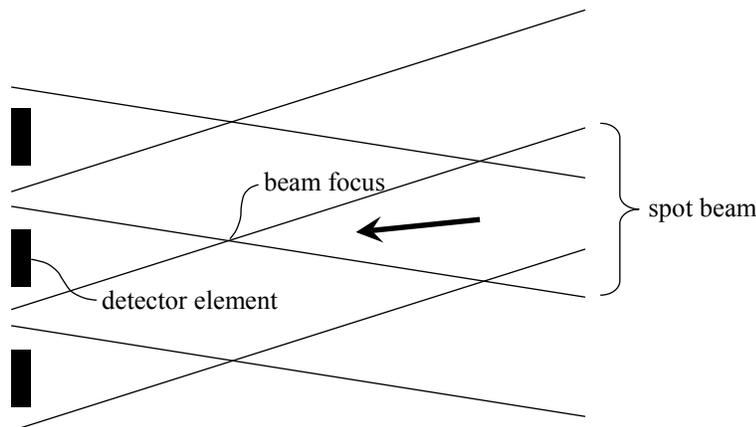
Figure 4. Detector array.

Referring back to Figure 1, the first projection system's aperture stop is at mirror **M2**, which can be an interchangeable element to accommodate alternative pupil functions (e.g., annular, dipole, etc.). A phase function such as a spiral-phase pattern can also be incorporated in the **M2** mirror topography. Alternatively, these types of pupil patterns can be incorporated in the microlens array, e.g. on **L1** in Figure 3, which would allow different source spots to have different pupil functions. A substantially achromatic spiral-phase pattern can be formed by combining phase-shift topographies on both **M2** and **L1**. (If necessary, a small field lens could be located at each intermediate lens focus to make **L1** exactly conjugate to the aperture stop.)

A spiral-phase pattern can greatly enhance image sensitivity to optical phase gradients in the mask reflectance. This imaging technique is described in "Spiral phase contrast imaging in microscopy", Optics Express Vol. 13, Issue 3, pp. 689-694 (2005), http://dx.doi.org/10.1364/OPEX.13.000689. In the present application, the spiral-phase pattern is formed as a modification of the mirror and/or microlens topography, which induces an optical phase shift that is a linear or staircase function of azimuth around each beam axis, and which varies from zero to 2π over the full azimuth range. The phase pattern induces an optical null along each beam axis, so if the detector array is configured to sense the axial beam intensities a dark-field image will result. A linear phase gradient in the mask reflectance at a particular image spot will induce a lateral translation of the optical intensity pattern on the corresponding detector element, so the optical null will be displaced and the detector signal will be high in the vicinity of phase gradients.

For a very small reflectance gradient the signal variation would be approximately proportional to the square of the gradient, but an alternative quadrant-detector technique can be used to obtain a signal that is approximately linear in the gradient, greatly increasing detection sensitivity. With this method, illustrated in Figure 5, each beam axis intercepts the corner point between four square detector elements **D1**, **D2**, **D3** and **D4** so that the optical null normally straddles all four elements symmetrically and the four corresponding detector signals are in balance. A lateral translation of the null resulting from a reflectance phase gradient will cause a signal imbalance that is approximately

proportional to the gradient. The signal differences between diagonally opposed detector elements (i.e., **D1** minus **D4**, or **D2** minus **D3**) provide a measure of the phase gradient's projection along the corresponding diagonal, and the two differences can be combined to define a vector representing the magnitude and direction of the phase gradient. The detector signals would similarly be sensitive to phase discontinuities and intensity variations in the mask reflectance.

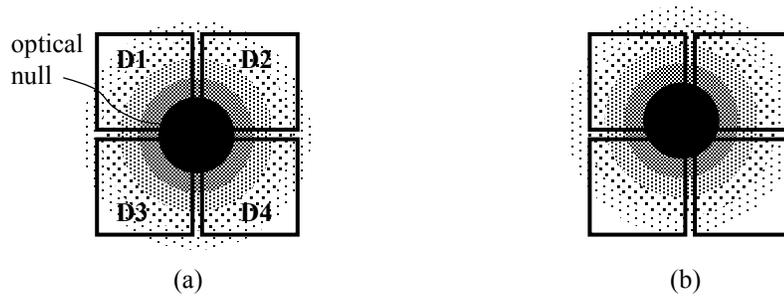|	
(a)	(b)

Figure 5. Quadrant detector with optical null symmetrically centered between the detector elements (a) and decentered (b).

In a variation of the Figure 1 system, the microlens and detector arrays can be combined into a single component, and a single projection system can be used to both illuminate and collect reflected radiation from the mask, as illustrated in Figure 6. This configuration uses an Offner projection system comprising two mirrors **M1** and **M2**. An expanded view of the combined microlens/detector array is illustrated in Figure 7. This system is more compact than Figure 1 and has the advantage that the microlens and detector arrays are automatically self-aligned. But it requires a custom-built detector array. The Figure 1 configuration could use an off-the-shelf EUV CCD, except that it may be difficult to achieve mechanical clearances between the two projection systems of Figure 1 if a large-format, 2-D CCD is used. The clearance limitation would not exist with the Figure 6 configuration.
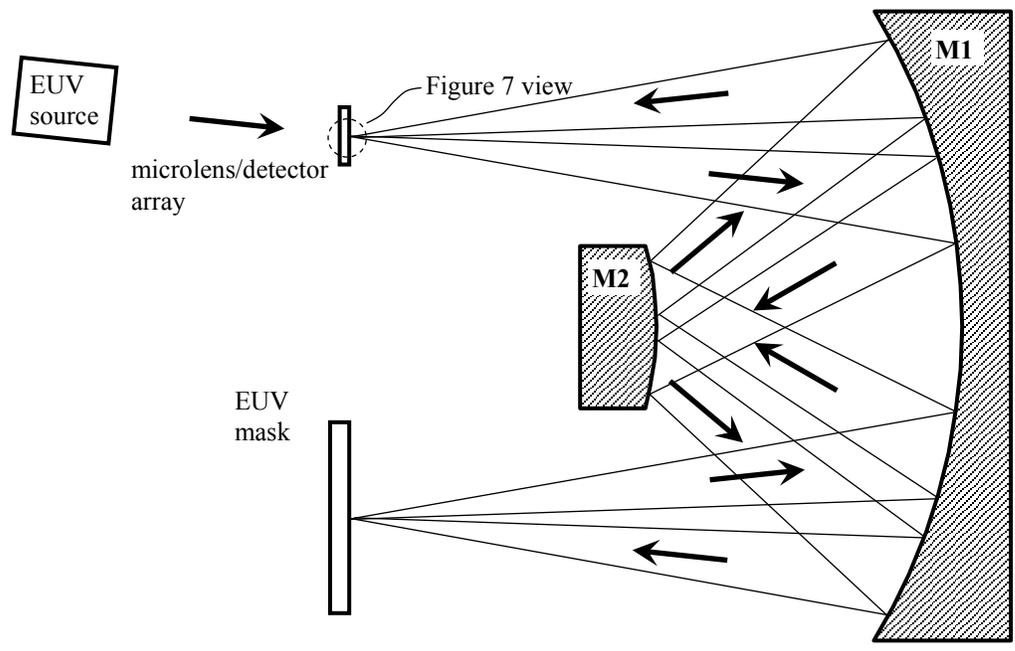
EUV
source

microlens/detector
array

Figure 7 view

M1

M2

EUV
mask

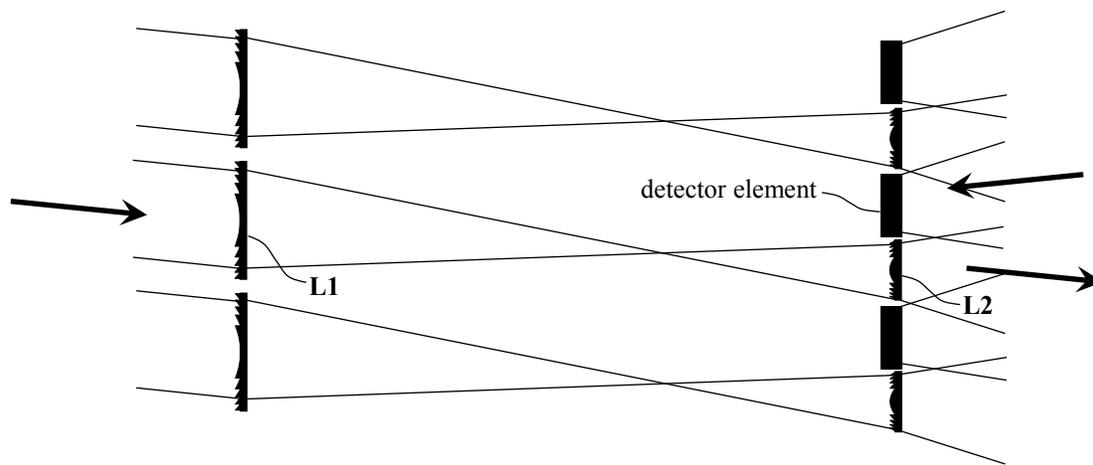Figure 6. Compact, self-aligned inspection system.

detector element

L1

L2

Figure 7. Combined microlens/detector array.